Biointerface Research in Applied Chemistry
Platinum Open Access Journal (ISSN: 2069-5837)

Article
Volume 11, Issue 4, 2021, 12082 - 12091
https://doi.org/10.33263/BRIAC114.1208212091

Antibacterial, Antifungal, Photocatalytic Activities and Seed Germination Effect of Mycosynthesized Silver Nanoparticles using *Fusarium oxysporum*

Khushbu Gupta [1], Tejpal Singh Chundawat [1,*], Nik Ahmad Nizam Nik Malek [2]

[1] The NorthCap University, India; khushbu.gupta30691@gmail.com (K.G.);
[2] Universiti Teknologi Malaysia (UTM), Malaysia; niknizam@utm.my (N.A.N.N.M.);
* Correspondence: chundawatchem@yahoo.co.in; (T.S.C);

Scopus Author ID 55428754800

Received: 30.11.2020; Revised: 29.12.2020; Accepted: 30.12.2020; Published: 2.01.2021

Abstract: The present research work is committed towards the green synthesis of silver nanoparticles (AgNP) using fungus *Fusarium oxysporum* and later analyzed for antibacterial, antifungal, photocatalytic activity, and enhancement of seed germination. The mycosynthesized AgNP were characterized by UV-Visible spectroscopy, Fourier Transform InfraRed (FTIR) spectroscopy, scanning electron microscopy (SEM), and X-ray diffraction (XRD). The UV-Visible spectra showed an absorption peak at 450 nm confirmed the formation of AgNP. A homogenous dispersion of spherical shape nanoparticles with a size of 40 nm was confirmed by SEM. The mycosynthesized AgNP affected bacteria more than a fungal strain. The AgNP could photo-catalytically degraded methylene blue. It enhanced seed germination of Vigna radiata (mung beans) appropriate conditions where the AgNP at 0.5 mg/ml can be utilized for growth improvement of commercially available crops. In conclusion, the AgNP can be synthesized by fungus *F. oxysporum* and potentially used as an antimicrobial agent, photocatalysis, and seed germination.

Keywords: silver nanoparticles; *Fusarium oxysporum*; antimicrobial activity; photocatalytic activity; vigna radiata; methylene blue.

1. Introduction

Nowadays, metal nanoparticles have emerged as the most promising scientific material because of their extraordinary biological and catalytic properties. Metallic nanoparticles have participated in various research applications and are found to be excellent heterogeneous catalysts [1-3]. Silver (Ag), owing to its stability, morphology, and surface charge, is one of the prominent materials used in nanotechnology research. To achieve monodispersity, the biological methods have emerged as the most suitable method for synthesizing silver nanoparticles (AgNP) over other chemical methods, such as by using bacteria [4], fungus [5-7], and plants [8-9].

A great threat to humanity and the environment has been caused by the quick appearance and re-appearance of multi-drug-resistant pathogens. [10]. To resist this problem, nanotechnology has been found to be useful as nanoparticles have a high surface to the volume ratio and less size imparts their antimicrobial activity [11, 12].

Methylene blue, a basic dye used for dyeing silk and wool, is also the major effluent of various industries' wastewater discharge. This non-degradable dye can cause harmful effects like diarrhea, nausea, vomiting, etc. [13]. Therefore, finding an effective treatment method for wastewater discharge becomes the need of the hour. Numerous techniques are available to remove such kinds of dyes, but in a recent scenario, metal nanoparticles were used to recover this problem. [14, 15]

Several research types demonstrated that metal nanoparticles positively influence nitrogen metabolism and photosynthesis, improving plant growth at low concentrations [16]. Seed germination is the key principle step in agriculture as it is the first stage in the plant growth process. The application of a different type of nanoparticles in the field of agriculture is rapidly increasing, and because of this, it is important to study the effect of AgNP in seed germination [17].

The present study's objective is to use endophytic fungus to bioreduce silver nitrate solution to AgNP and assess its bioefficacy for its effective use in the field of environment, agriculture, and pharmaceutical industry (Figure 1).

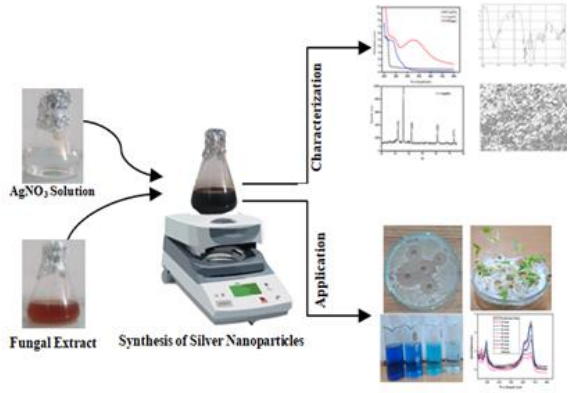

Figure 1. Fungal mediated synthesis of metal nanoparticles and their applications.

2. Materials and Methods

2.1. Collection of material.

Nutrient agar, potato dextrose agar (PDA), silver nitrate ($AgNO_3$), peptone, beef extract, Sodium chloride (NaCl), yeast extract, and Czapek dox agar were purchased from Sigma Aldrich. Seeds of *Vigna radiata* (mung beans) were collected from the local market of Gurugram, Haryana.

2.2. Test organisms.

Klebsiella pneumonia (MTCC 109), *Staphylococcus aureus* (MTCC 96), *Pseudomonas aeruginosa* (MTCC 441), *Escherichia coli* (MTCC 442), and *Aspergillus niger* (MTCC 282) were used as test microbes that were procured from Microbial Type Culture Collection (MTCC), India.

2.3. Preparation of fungal extract and biogenic synthesis of silver nanoparticles.

The PDA medium was used for the growth of fungus *Fusarium oxysporum* at 28 °C. This was then inoculated in the MGYP medium with 2% malt extract, 11% glucose, 5% yeast extract, and 10% peptone. The culture was incubated for 7 days with agitation at 28°C and

later, centrifuged to collect biomass and finally washed three times with distilled water. After that, 10.0 g of the biomass was incubated with 100 ml distilled water for 72 h at 28°C. The fungal extract was prepared by filtration using Whatman Filter paper No. 1 and then stored in the refrigerator at 4°C for further experimental usage. $AgNO_3$ was added to this filtrate to make an overall solution of 10^{-3} M in a 250ml Erlenmeyer flask. The mixture was stirred using a magnetic stirrer for 2 h at normal room temperature. The reaction progress was continuously monitored by observing color changes from pale yellow to dark brown.

2.4. Characterization of AgNPs.

The synthesized nanoparticles' characterization is an essential part of the assurance of shape, size, morphology, phase purity, and surface charge. To confirm the reduction of Ag^+ ions into Ag^0, the solution was analyzed using a UV-Visible spectrophotometer (Cary series) from 200-800 nm and using distilled water as a blank sample. The morphology and size of the synthesized nanoparticles were analyzed by scanning electron microscope (Model-FEI Quanta 200 SEM). Fourier transform infrared spectra (FTIR) spectroscopic analysis of biosynthesized AgNP was recorded using FTIR (Perkin Elmer) using the KBr pellet technique in the range of 400-4000 cm^{-1}. The crystal structure, particle size, and phase identification of metal nanoparticles were analyzed using Philips Expert pro-X-ray diffraction (XRD) system (DY 1650) at 2θ angle ranging from 20-90°.

2.5. Antimicrobial assay.

The antimicrobial activity of the biosynthesized AgNPs was studied against five different pathogenic strains which are *Klebsiella pneumonia* (MTCC 109), *Escherichia coli* (MTCC 442), Pseudomonas *aeruginosa* (MTCC 441), *Staphylococcus aureus* (MTCC 96), and *Aspergillus niger* (MTCC 282) using agar well plate technique. All four bacterial strains were grown in nutrient agar (NA) media consisting of 1 L of distilled water containing 2.0 g yeast extract, 5.0 g peptone, 10.0 g beef extract, 5.0 g NaCl, and 15.0 g agar. The fungus *A. niger* was grown using Czapek dox extract agar. The autoclaved NA agar was poured on Petri plates and allowed to solidify. The L-spreader was used to spread the culture on Petri plates. The agar wells were punched (8 mm) with sterile micropipette tips and loaded with the test solution (AgNPs). The plates were then incubated overnight, and the diameter of the zone of inhibition was recorded in millimeters. Double distilled water, fungal extract, and DMSO (Dimethyl sulfoxide) was added as a negative control. Drugs such as chloramphenicol and ampicillin (in case of bacteria) along with Nystatin and Griseofulvin (in case of fungus) were used as a positive control to evaluate the potency of tested compounds under the same conditions. Each experiment was done in triplicates to get an average value. Minimum inhibitory concentration was determined for all the compounds using the agar dilution method by making different dilutions of AgNP by DMSO such as 250, 120, 62.5, 100, 50, 25, and 12.5µg/ml. The maximum dilution showing nearly 99% inhibition was selected as MIC value [18, 19].

2.6. Photocatalytic degradation of methylene blue.

The photocatalytic activity of the biosynthesized AgNP was studied during midday against methylene blue dye under direct sunlight (30 Klux). Methylene blue is a heterocyclic aromatic chemical compound with molecular formula $C_{16}H_{18}N_3SCl$. The absorption peak for methylene blue dye in water was centered at 664 nm, and the other two small absorption peaks

were at 293 and 243nm in the UV-Visible spectrum. The decay of dye methylene blue was evident from a gradual decrease in the dye's absorption intensity. About 10 mg of the AgNP were added to 50 ml methylene blue dye solution (10^{-5} M). The mixture was stirred for 30 min to obtain equilibrium between absorption and desorption. At a regular interval of time, 5 ml of the solution was taken and centrifuged immediately to remove all AgNP and analyzed using UV-Vis spectrophotometer.

2.7. Effect on seed germination.

2.7.1. Preparation of AgNPs suspension.

The stock suspension of AgNP was prepared by mixing AgNP in double-distilled water. The mixture was ultrasonicated for 30 min for a proper agitation of AgNP suspension. According to the method of Zang *et al.* [20], 10% polyethylene glycol (PEG) was further added to stabilize the AgNPs suspension. The final suspension of AgNP was again stirred before further use.

2.7.2. Effect on seed germination of *Vigna radiata.*

Seeds of *V. radiata* (mung beans) were first washed with teepol and then immersed in a 5% sodium hypochlorite solution to ensure their surface sterility. Seeds were then washed 2-3 times with sterilized double-distilled water under laminar airflow. The seeds were then soaked in double-distilled water for 2 h and again for 1 h at different concentrations of AgNP. About 3-4 stack of filter paper was put into each petri dish. The seeds were then transferred into a Petri dish with 10 seeds per dish at a distance of 1 cm between them. Petri dishes were covered and were maintained at 26 ±2°C and illuminated with 8 hours light and 16 hours dark in the culture room. For morphological studies, the time of germination was permitted up to 72 h, and pictures were taken. A petri dish without AgNP was used as a control sample.

3. Results and Discussion

3.1. Characterization of mycosynthesized AgNP.

The UV-Visible spectra of AgNPs synthesized using the fungus *Fusarium oxysporum* is shown in Figure 2. In silver nanoparticles, valance and conduction band are present near each other, through which electrons can jump easily.

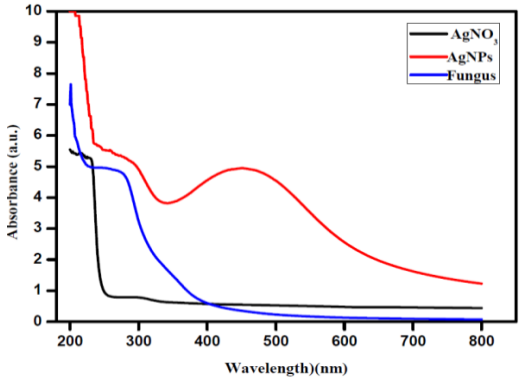

Figure 2. UV-Vis absorption spectra of $AgNO_3$, fungal extracts, and AgNPs.

These free electrons are responsible for the surface plasmon resonance (SPR) absorption band, occurring due to the mutual vibration of silver nanoparticles' electrons in

resonance with light-wave. The absorption peak was obtained at 450 nm confirmed the synthesis of AgNp. The stability of synthesized nanoparticles was observed for 3 months, and the peak was found to be the same at 450 nm. [20, 21].

FTIR readings were taken to find out the accountable functional groups for reducing silver ions and stabilization and capping of mycosynthesized silver nanoparticles. The standard values were compared with observed peaks for functional group identification. Different peaks located at 3305.99, 2927.94, 1693, 1650, 1553, 1375, 1147, 1076, 1043 cm^{-1} were found in spectra of *Fusarium oxysporum* (Figure 3).

The band at 3305.99 cm^{-1} corresponds to N-H and O-H stretching showing phenol and alcohol presence. The band at position 2927.94 cm^{-1} arising from Lipids asymmetric CH_2 stretching were observed. FTIR spectrum reveals two bands at 1650 and 1553 cm^{-1} that correspond to the bending vibrations of the amide I and amide II bands of the proteins, respectively. The band at 1375.25 and 1147.65 cm^{-1} in the FTIR spectra represents the C–N and C–C stretching, which indicates the existence of proteins and carbohydrates. The peak at 1076 cm^{-1} appears due to nucleic acid and carbohydrate vibrations [22]. The peak at 1076 cm^{-1} represents C-OH coupled with bending [23-25].

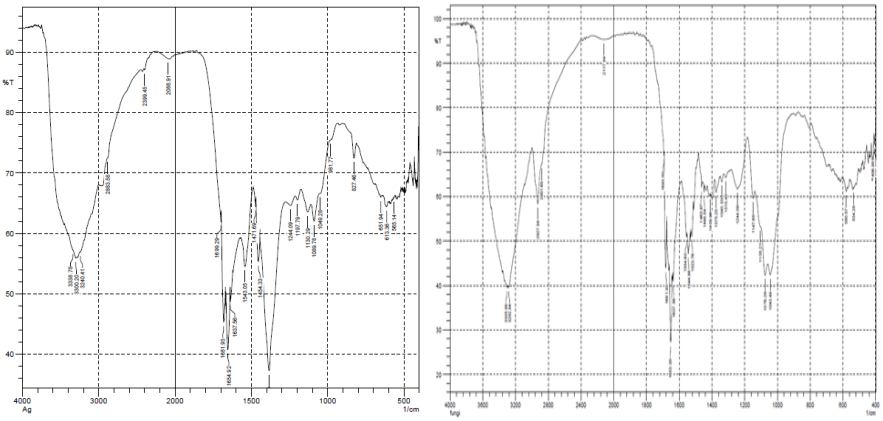

Figure 3. FTIR spectra of silver nanoparticles and *Fusarium oxysporum.*

X-ray crystallography was used to confirm the crystalline nature of nanoparticles. The typical XRD pattern for AgNPs, prepared by the given biological method, is shown in Figure 4. The particle size was calculated by the Debye Scherrer formula, Where 'λ' is the wavelength of X-Ray (0.1541 nm), 'W' is FWHM (full width at half maximum), 'θ' is the diffraction angle and 'D' is particle diameter (size). The average particle size was calculated to be around 42 nm. Table 1 gives the diffraction planes, FWHM, and d-spacing [25].

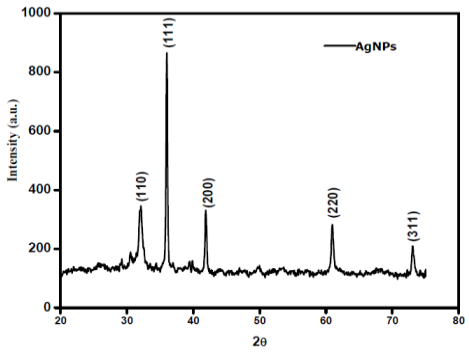

Figure 4. XRD patterns of AgNPs.

$$D = \frac{0.9\lambda}{\beta\cos\theta}$$

$2\Theta = 36.05$

$\beta = 0.281 \times 3.14 \div 180 = 0.00490$

$$D = \frac{0.9 \text{ x } 0.1541}{0.00490 \text{ x } \text{Cos}18.025} = 42\text{nm}$$

Table 1. XRD results of silver nanoparticles.

Diffraction Angle	FWHM	d- spacing	Diffraction plane
32.03	1.33	0.279	110
36.05	0.281	0.2491	111
41.91	0.481	0.2153	200
60.94	0.80	0.1518	220
73.02	1.907	0.1295	311

The SEM image of the synthesized nanoparticles is given in Figure 5. The SEM image showed that silver nanoparticles have smooth morphology with a spherical shape. The nanoparticles' diameter was observed to be around 40nm. The SEM image also demonstrated that the synthesized nanoparticles were more or less uniform in shape and size [26].

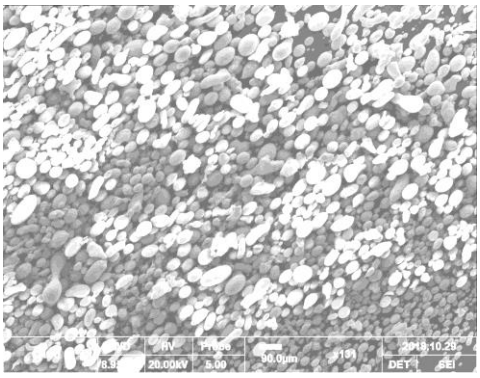

Figure 5. SEM image of silver particles.

3.2. Antimicrobial activity of AgNPs.

The well filled with DMSO, fungal extract, and distilled water did not show any inhibition zone, but the wells filled with newly synthesized compounds show antimicrobial activity for both bacterial strains (Gram-negative and Gram-positive) and fungal strain ranging from 8-24 mm (Figure 6). It is noteworthy that newly synthesized silver nanoparticles were more active towards bacteria as compared to fungus. Silver nanoparticles were even more potent than commercially available drugs in the market (Figure 7) [27].

Figure 6. Antibacterial effect of synthesized silver nanoparticles against *Staphylococcus aureus.*

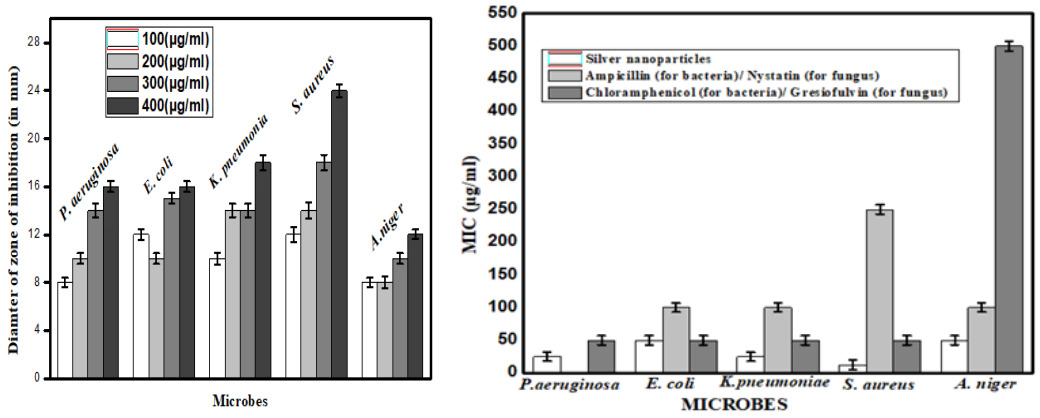

Figure 7. Diameter of zone of inhibition & Minimum inhibitory concentration against microbes.

3.3. Photocatalytic degradation.

The experiments were conducted by varying the catalyst dose range from 0.05 to 0.2 g and keeping the other experimental conditions constant. The degradation of the methylene blue dye increases linearly with an increase in the catalyst dose, but the best results were obtained at 0.1g. The reaction's progress was monitored by a UV-visible spectrophotometer by measuring the absorption intensity of the dye at a different time interval. Two controlled sets were maintained without AgNPs and with the fungal extract. Absorbance was measured from time to time. No major degradation was observed in both sets than silver nanoparticles (Figure 8) [28-30].

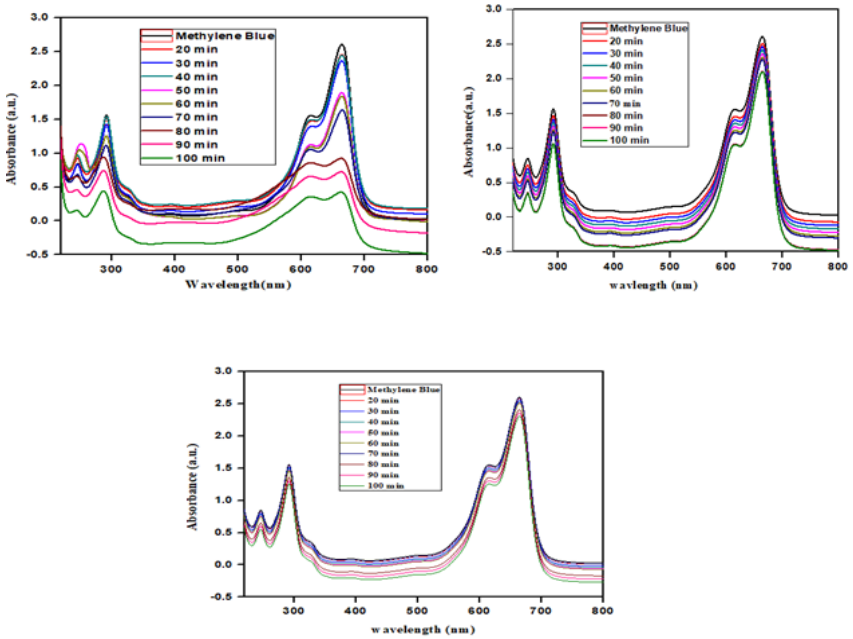

Figure 8. UV-Vis spectra of methylene blue dye with time (a) With AgNPs (b) With extract of *Fusarium oxysporum* (c) in the absence of AgNPs.

3.4. Enhancement of seed germination.

Seed germination was found to be effective in plant growth, yield, and development (Figure 9). In this study, among the four different concentration (0.5mg/l, 1mg/l, 1.5mg/ml, 2 mg/ml), 0.5mg/ml showed highest germination percent followed by 1mg/ml and 1.5mg/ml. However, at 2mg/ml concentration, nanoparticles inhibit the growth of mung bean seeds [17].

Figure 9. Growth of Vigna radiata with (a) silver nanoparticles (b) without nanoparticles.

4. Conclusions

The immediate study revealed an environment-friendly method for forming silver nanoparticles by using the fungus *Fusarium oxysporum*. Here the extract of fungus *Fusarium oxysporum* acts as both a reducing and stabilizing agent. The synthesized silver nanoparticles were characterized by UV- Visible spectroscopy, FTIR, SEM, and XRD. These nanoparticles also possess a powerful absorption spectrum in visible range due to their surface prrytlasmon resonance. The functional groups responsible for reduction and stabilization were confirmed by FTIR. The XRD pattern showed an FCC crystal structure. The SEM results revealed that nanoparticles were pure, spherical in shape, along with a size range of 40–60 nm. The biosynthesized AgNPs were found to have pronounced antimicrobial activity against both bacteria and fungus. Furthermore, synthesized silver nanoparticles showed excellent photocatalytic activity against methylene blue dye and Vigna radiata seeds' germination ability.

Funding

This research received no external funding.

Acknowledgments

The authors are thankful to the Department of Biotechnology (DBT) for providing financial support in terms of fellowship to Ms. Khushbu Gupta. We are also thankful to the Guru Jambheshwar University of Science and Technology, Hisar, for the instrumentation facility of X-ray diffraction analysis and Fourier Transform Infrared Spectroscopy.

Conflicts of Interest

There is no conflict of interest.

References

1. Bayda, S.; Adeel, M.; Tuccinardi, T.; Cordani, M.; Rizzolio, F. The history of nanoscience and nanotechnology: From chemical–physical applications to nanomedicine. *Molecules* **2020**, *25*, https://doi.org/10.3390/molecules25010112.
2. Srinoi, P.; Chen, Y.T.; Vittur, V.; Marquez, M.D.; Lee, T.R. Bimetallic nanoparticles: enhanced magnetic and optical properties for emerging biological applications. *Applied Sciences* **2018**, *8*, https://doi.org/10.3390/app8071106.
3. Gupta, K.; Chundawat, T.S. Zinc oxide nanoparticles synthesized using Fusarium oxysporum to enhance bioethanol production from rice-straw. *Biomass and Bioenergy* **2020**, *143*, https://doi.org/10.1016/j.biombioe.2020.105840.
4. Saifuddin, N.; Wong, C. W.; Yasumira, A. A. Rapid biosynthesis of silver nanoparticles using culture supernatant of bacteria with microwave irradiation. *E J Chem.* **2009**, *6*, 61-70, https://doi.org/10.1155/2009/734264.

5. Ramos, M.M.; Morais, E.D.S.; Sena, I.D.S.; Lima, A.L.; de Oliveira, F.R.; de Freitas, C.M.; Fernandes, C.P.; de Carvalho, J.C.T.; Ferreira, I.M. Silver nanoparticle from whole cells of the fungi Trichoderma spp. isolated from Brazilian Amazon. *Biotechnol. Letters* **2020**, *42*, 1-11, https://doi.org/10.1007/s10529-020-02819-y.
6. Guilger-Casagrande, M.; de Lima, R. Synthesis of silver nanoparticles mediated by fungi: A Review. *Frontiers in bioengineering and biotechnology* **2019,** *7*, https://doi.org/10.3389/fbioe.2019.00287.
7. Birla, S.S.; Gaikwad, S.C.; Gade, A.K.; Rai, M.K. Rapid synthesis of silver nanoparticles from Fusarium oxysporum by optimizing physicocultural conditions. *Science World Journal*. **2013**, *2013*, 1-12, https://doi.org/10.1155/2013/796018.
8. Wei, S.; Wang, Y.; Tang, Z.; Hu, J.; Su, R.; Lin, J.; Zhou, T.; Guo, H.; Wang, N.; Xu, R. A size-controlled green synthesis of silver nanoparticles by using the berry extract of Sea Buckthorn and their biological activities. *New J Chem* **2020**, *44*, 9304-9312, https://doi.org/10.1039/D0NJ01335H.
9. Yousaf, H.; Mehmood, A.; Ahmad, K.S.; Raffi, M. Green synthesis of silver nanoparticles and their applications as an alternative antibacterial and antioxidant agents. *Mater. Sci Eng. C*. **2020**, *112*, https://doi.org/10.1016/j.msec.2020.110901.
10. Yusuf, M. Silver Nanoparticles: Synthesis and Applications. *Handbook of Ecomaterials* **2019**, 2343–2356, https://doi.org/10.1007/978-3-319-68255-6_16.
11. Garibo, D.; Borbón-Nuñez, H.A.; de León, J.N.D.; Mendoza, E.G.; Estrada, I.; Toledano-Magaña, Y.; Tiznado, H.; Ovalle-Marroquin, M.; Soto-Ramos, A.G.; Blanco, A.; Rodríguez, J.A. Green synthesis of silver nanoparticles using Lysiloma acapulcensis exhibit high-antimicrobial activity. *Scientific reports*. **2020,** *10*, 1-11, https://doi.org/10.1038/s41598-020-69606-7.
12. Arya, A.; Gupta, K.; Chundawat, T.S. In Vitro Antimicrobial and Antioxidant activity of Biogenically Synthesized Palladium and Platinum Nanoparticles using Botryococcus braunii. *TJPS* **2019**, *1*, 1-21. https://doi.org/10.4274/tjps.galenos.2019.94103.
13. Mohamed, R.M.; Mkhalid, I.A.; Baeissa, E S.; Al-Rayyani, M.A. Photocatalytic degradation of methylene blue by Fe/ZnO/SiO2 nanoparticles under visible light. *J Nanotecnol*. **2012**, *2012*, https://doi.org/10.1155/2012/329082.
14. Gupta, K.; Chundawat, T.S. Bio-inspired synthesis of platinum nanoparticles from fungus Fusarium oxysporum: its characteristics, potential antimicrobial, antioxidant and photocatalytic activities. *Mater Res Express*. **2019**, *6*, https://doi.org/10.1088/2053-1591/ab4219.
15. Salehi, M.; Hashemipour, H.; Mirzaee, M. Experimental study of influencing factors and kinetics in catalytic removal of methylene blue with TiO2 nanopowder. *Am J Environ Eng*. **2012**, *2*, 1-7, https://doi.org/10.5923/j.ajee.20120201.01.
16. Sadak, M.S. Impact of silver nanoparticles on plant growth, some biochemical aspects, and yield of fenugreek plant (Trigonella foenum-graecum*). Bull. Natl. Res. Cent.* **2019** *43*, https://doi.org/10.1186/s42269-019-0077-y.
17. Bose, P.; Gowrie, S.U. Mycosynthesis, Optimisation and Characterization of Silver Nanoparticles by Endophytic Fungus Isolated from the Root of Casuarina junghuhniana. *Miq. Int J Pharm Sci Rev Res* **2017**, *43*, 107-115.
18. Arya, A.; Gupta, K.; Chundawat, T.S.; Vaya, D. Biogenic synthesis of copper and silver nanoparticles using green alga Botryococcus braunii and its antimicrobial activity. *Bioinorg Chem Appl* **2018**, *2018*, 1-9, https://doi.org/10.1155/2018/7879403.
19. Ishida, K.; Cipriano, T.F.; Rocha, G.M.; Weissmüller, G.; Gomes, F.; Miranda, K.; Rozental, S. Silver nanoparticle production by the fungus Fusarium oxysporum: nanoparticle characterisation and analysis of antifungal activity against pathogenic yeasts. *Memórias do Instituto Oswaldo Cruz* **2014,** *109*, 220-228, https://doi.org/10.1590/0074-0276130269.
20. Nilavukkarasi, M.; Vijayakumar, S.; Kumar, S.P. Biological synthesis and characterization of silver nanoparticles with Capparis zeylanica L. leaf extract for potent antimicrobial and anti proliferation efficiency. *Materials Science for Energy Technologies* **2020**, *3*, 371-376, https://doi.org/10.1016/j.mset.2020.02.008.
21. Devaraj, P.; Kumari, P.; Aarti, C.; Renganathan, A. Synthesis and characterization of silver nanoparticles using cannonball leaves and their cytotoxic activity against MCF-7 cell line. *J Nanotechnol* **2013**, *2013*, https://doi.org/10.1155/2013/598328.
22. Salman, A.; Pomerantz, A.; Tsror, L.; Lapidot, I.; Zwielly, A.; Moreh, R.; Mordechai, S.; Huleihel, M Distinction of Fusarium oxysporum fungal isolates (strains) using FTIR-ATR spectroscopy and advanced statistical methods. *The Analyst.* **2011,** *136*, 988-995, https://doi.org/10.1155/2012/109708.
23. Karthik, C.; Suresh, S.; Sneha Mirulalini, G.; Kavitha, S. A FTIR approach of green synthesized silver nanoparticles by *Ocimum sanctum* and Ocimum gratissimum on mung bean seeds. *Inorganic and Nano-Metal Chemistry* **2020** *1–7*, https://doi.org/10.1080/24701556.2020.1723025.
24. Salman, A.; Tsror, L.; Pomerantz, A.; Moreh, R.; Mordechai, S.; Huleihel, M. FTIR spectroscopy for detection and identification of fungal phytopathogenes. *Spectroscopy* **2010**, *24*, 261-267, https://doi.org/10.3233/SPE-2010-0448.

25. Anandalakshmi K.; Venugobal, J.; Ramasamy, V. Characterization of silver nanoparticles by green synthesis method using Pedalium murex leaf extract and their antibacterial activity. *App Nanosci* **2015**, *6*, 399–408, https://doi.org/10.1007/s13204-015-0449-z.
26. Jyoti, K.; Baunthiyal, M.; Singh, A. Characterization of silver nanoparticles synthesized using Urtica dioica Linn. leaves and their synergistic effects with antibiotics. *J Radiat Res App Sci* **2016**, *9*, 217-227, https://doi.org/10.1016/j.jrras.2015.10.002.
27. Kambale, E.K.; Nkanga, C.I.; Mutonkole, B.P.I.; Bapolisi, A.M.; Tassa, D.O.; Liesse, J.M.I.; Krause, R.W.; Memvanga, P.B. Green synthesis of antimicrobial silver nanoparticles using aqueous leaf extracts from three Congolese plant species (Brillantaisia patula, Crossopteryx febrifuga and Senna siamea). *Heliyon* **2020**, *6*, https://doi.org/10.1016/j.heliyon.2020.e04493.
28. Marimuthu, S.; Antonisamy, A.J.; Malayandi, S.; Rajendran, K.; Tsai, P.C.; Pugazhendhi, A.; Ponnusamy, V.K. Silver nanoparticles in dye effluent treatment: A review on synthesis, treatment methods, mechanisms, photocatalytic degradation, toxic effects and mitigation of toxicity. *J Photochem Photobiol B* **2020**, *205*, https://doi.org/10.1016/j.jphotobiol.2020.111823.
29. Vanaja, M.; Paulkumar, K.; Baburaja, M.; Rajeshkumar, S.; Gnanajobitha, G.; Malarkodi, C.; Sivakavinesan, M.; Annadurai, G. Degradation of methylene blue using biologically synthesized silver nanoparticles. *Bioinorg Chem Appl*. **2014**, *2014*, 1-8, https://doi.org/10.1155/2014/742346.
30. Aboelfetoh, E.F.; Gemeay, A.H.; El-Sharkawy, R.G. Effective disposal of methylene blue using green immobilized silver nanoparticles on graphene oxide and reduced graphene oxide sheets through one-pot synthesis. *Environmental Monitoring and Assessment* **2020**, *192*, 1-20, https://doi.org/10.1007/s10661-020-08278-2.